Electronic Supplementary Material (ESI) for ChemComm.
This journal is © The Royal Society of Chemistry 2014

# Supporting Information for:

# Sulfated quaternary amine lipids: a new class of inverse charge zwitterlipids

Vincent J. Venditto,[a] Aaron Dolor,[a] Aditya Kohli,[b] Stefan Salentinig,[c] Ben J. Boyd[c] and Francis C. Szoka, Jr.[a,b]

[a]Department of Bioengineering and Therapeutic Sciences, School of Pharmacy, University of California San Francisco, San Francisco, CA 94143. [b]The UC Berkeley-UCSF Graduate Program in Bioengineering, University of California Berkeley, Berkeley, CA 94720. [c]Drug Delivery, Disposition and Dynamics, Monash Insititute of Pharmaceutical Sciences, Monash University, Victoria 3052, Australia.

This work was supported by NIH EB003008. VJ Venditto was funded by a grant from the National Institutes of Allergy and Infectious diseases of the National Institutes of Health under Award Number F32AI095062. A Dolor was funded by a fellowship from the National Science Foundation Graduate Research Fellowship Program. The content is solely the responsibility of the authors and does not necessarily represent the official views of the National Institutes of Health or the National Science foundation.

Address correspondence and reprint requests to Dr. Francis C. Szoka, Jr., Departments of Bioengineering and Therapeutic Sciences and Pharmaceutical Chemistry, School of Pharmacy, University of California, San Francisco, San Francisco, California, 94143-0912. Tel: (415) 476-3895; Fax: (415) 476-0688; E-mail: szoka@cgl.ucsf.edu.

**Table of Contents**

## Experimental Section

1. Materials.

NMR measurements were performed on a Bruker (Billerica, MA) 300MHz Avance system and analyzed using TopSpin software. Chemical shifts are expressed as parts per million using tetramethylsilane or $CDCl_3$ solvent peaks as internal standards. MALDI-TOF measurements were performed on a Bruker Daltonics MicroFlex LT system (Billerica, MA). High Performance flash chromatography (HPFC) was carried out using a Grace Reveleris Flash System (Columbia, MD) with prepacked silica gel columns. Elemental analysis was performed by the Microanalytical Laboratory at the University of California Berkeley using an ICP Optima 7000 DV instrument. Zeta potential and size measurements were carried out using a Nano-ZS Dynamic Light Scattering Instrument from Malvern (Westborough, MA). Differential Scanning Calorimetry (DSC) measurements were obtained using a high temperature MC-DSC 4100 calorimeter from Calorimetry Sciences Corp. (Lindonk, UT). Fluorescence measurements were made on a FLUOstar plate reader from BMG Labtech (Durham, NC) with excitation at 485 nm and emission at 518 nm. TEM images were obtained using an FEI Tecnai 12 transmission electron microscope at the University of California Berkeley Robert D. Ogg Electron Microscope Laboratory or the University of California, San Francisco Molecular Electron Microscopy Lab.

2. General Synthetic Scheme.

Lipids were prepared in a two-step synthesis (Scheme 1) starting with the acylation of 3-(dimethylamino)-1,2-propanediol as previously reported (Kohli, 2012). Synthesis of 1-bromo-3-propanesulfate (**1**) was performed by stirring 1 mmol of 1-bromo-3-propanol at 0.2 M in DCM as 4 mmol sulfurtrioxide-pyridine complex (45%) and 1 mmol diisopropyl ethylamine was added. The

reaction was then heated to 40 °C overnight under nitrogen. The reaction was concentrated and taken up in DCM to afford a solid, which was removed by filtration and the filtrate purified by silica gel flash chromatography (0-10% methanol in DCM). The product eluted as the 1-bromo-3-propanesulfate – diisopropyl ethylamine salt in a 1:1 ratio as determined by NMR.

The diacyl tertiary amine lipid (**2a-f**) (1 mmol) was then quaternized with 1-bromo-3-propanesulfate (**1**) (3.5 mmol) and 2 mmol diisopropyl ethylamine in dimethylformamide at 0.15 M. The reactions were heated to 60 °C overnight under nitrogen. A precipitate formed in the reactions with saturated lipid tails (distearoyl (**3b**), dipalmitoyl (**3c**), dimyristoyl (**3d**), dilauryl (**3e**) and dicapryloyl (**3f**)) and these solutions were then heated to 80 °C for 2 hours before cooling to room temperature. The precipitate reformed and was filtered and washed with DMF to yield a white solid. Quaternization of the unsaturated lipid (dioleoyl (**3a**)) was performed in the same manner, but did not result in a precipitate. The reaction mixture was concentrated and taken up in DCM and purified by silica gel flash chromatography (0-10% methanol in chloroform with 0.1% $NH_4OH$).

3. Chemical Characterization.

**1-bromo-3-propanesulfate – diisopropyl ethylamine salt (1)**. Yield (74%). $^1$H NMR (CDCl3): δ 1.44 (*d*, 6H, DIPEA), 1.51 (*d*, 6H, DIPEA), 1.51 (*d*, 6H, DIPEA), 1.53 (*t*, 3H, DIPEA), 2.24 (*tt*, 2H), 2.24 (*tt*, 2H), 3.13 (*m*, 2H, DIPEA), 3.54 (t, 2H), 3.69 (*m*, 2H, DIPEA), 4.19 (t, 2H). $^{13}$C NMR (CDCl3): δ 12.4 (DIPEA), 17.3 (DIPEA), 18.6 (DIPEA), 30.2, 32.7, 42.8 (DIPEA), 54.5 (DIPEA), 65.3.

**DOAS (3a)**. Yield: 45%. $^1$H NMR ($CDCl_3$): δ 0.89 (*t*, 6H), 1.29 (*m*, 40H), 1.59 (*m*, 4H), 2.02 (m, 8H), 2.26 (*m*, 2H), 2.32 (*m*, 4H), 3.21 (*s*, 3H), 3.28 (*s*, 3H), 3.49 (*m*, 2H), 3.68 (*t*, 2H), 3.94 (*dd*, 1H), 4.12 (*t*, 2H), 4.51 (*dd*, 1H), 5.35 (*m*, 4H), 5.64 (*m*, 1H). $^{13}$C NMR (CDCl3): δ 14.12, 22.68, 24.70, 24.80, 27.22, 27.24, 29.10, 29.16, 29.20, 29.22, 29.28, 29.32, 29.34, 29.54, 29.78, 31.91, 33.89, 34.19, 51.18,

51.63, 63.37, 65.81, 129.70, 130.05, 172.80, 173.23. MALDI-TOF calculated for [$C_{44}H_{83}NO_8S$] (m/z): 785.58, observed: 787.39. Elemental analysis for [$C_{44}H_{83}NO_8S$]: C, 67.22; H, 10.64; N, 1.78; S, 4.08. Found: C, 67.22; H, 10.90; N, 1.68; S, 4.33.

**DSAS (3b)**. Yield: 42%. $^1$H NMR ($CDCl_3$:MeOD (20:1)): δ 0.76 (*t*, 6H), 1.14 (*m*, 56H), 1.49 (*m*, 4H), 2.06 (*m*, 2H), 2.24 (*m*, 4H), 2.99 (*s*, 3H), 3.03 (*s*, 3H), 3.49 (*m*, 2H), 3.57 (*t*, 2H), 3.93 (*dd*, 1H), 4.00 (*t*, 2H), 4.34 (*dd*, 1H), 5.48 (*m*, 1H). $^{13}$C NMR (CDCl3): δ 13.60, 22.31, 24.30, 24.38, 25.28, 28.77, 29.00, 29.16, 29.33, 31.57, 33.49, 33.75, 50.51, 51.25, 57.60, 62.95, 63.54, 63.83, 65.18, 172.65, 173.23. MALDI-TOF calculated for [$C_{44}H_{87}NO_8S$] (m/z): 789.62, observed: [M+H] 791.16. Elemental analysis for [$C_{44}H_{87}NO_8S$]: C, 66.79; H, 11.21; N, 1.77; S, 4.05. Found: C, 66.58; H, 11.54; N, 1.74; S, 4.65. Note: Elemental analysis of sulfur is believed to be high due to free sulfate.

**DPAS (3c)**. Yield: 71%. $^1$H NMR ($CDCl_3$:MeOD (20:1)): δ 0.79 (*t*, 6H), 1.17 (*m*, 48H), 1.52 (*m*, 4H), 2.09 (*m*, 2H), 2.26 (*m*, 4H), 3.01 (*s*, 3H), 3.05 (*s*, 3H), 3.51 (*m*, 2H), 3.61 (*t*, 2H), 3.95 (*dd*, 1H), 4.03 (*t*, 2H), 4.35 (*dd*, 1H), 5.51 (*m*, 1H). $^{13}$C NMR (CDCl3): δ 13.95, 22.57, 22.85, 24.56, 24.63, 29.00, 29.04, 29.22, 29.26, 29.43, 29.55, 29.57, 29.59, 31.82, 33.74, 34.03, 50.82, 51.34, 57.98, 63.22, 63.79, 63.90, 64.22, 64.39, 65.48, 172.86, 173.41. MALDI-TOF calculated for [$C_{40}H_{79}NO_8S$] (m/z): 733.55, observed: [M+H] 734.88. Elemental analysis for [$C_{40}H_{79}NO_8S$]: C, 65.35; H, 10.97; N, 1.91; S, 4.36. Found: C, 65.17; H, 11.33; N, 1.95; S, 4.79.

**DMAS (3d)**. Yield: 71%. $^1$H NMR ($CDCl_3$:MeOD (20:1)): δ 0.82 (*t*, 6H), 1.20 (*m*, 40H), 1.53 (*m*, 4H), 2.14 (*m*, 2H), 2.29 (*m*, 4H), 3.05 (*s*, 3H), 3.10 (*s*, 3H), 3.56 (*m*, 2H), 3.67 (*t*, 2H), 3.99 (*dd*, 1H), 4.06 (*t*, 2H), 4.38 (*dd*, 1H), 5.53 (*m*, 1H). $^{13}$C NMR (CDCl3): δ 13.89, 22.51, 22.81, 24.50, 24.57, 28.97, 29.19, 29.35, 29.49, 31.76, 33.68, 33.97, 50.66, 51.22, 63.09, 63.61, 63.88, 64.47, 65.37, 172.75, 173.31. MALDI-TOF calculated for [$C_{36}H_{71}NO_8S$] (m/z): 677.49, observed: [M+H] 678.59. Elemental analysis

for [$C_{36}H_{71}NO_8S$]: C, 63.68; H, 10.69; N, 2.06; S, 4.72. Found: C, 63.52; H, 10.92; N, 1.98; S, 5.35. Note: Elemental analysis of sulfur is believed to be high due to free sulfate.

**DLAS (3e)**. Yield: 69%. $^1$H NMR ($CDCl_3$:MeOD (20:1)): δ 0.77 (*t*, 6H), 1.15 (*m*, 32H), 1.50 (*m*, 4H), 2.07 (*m*, 2H), 2.24 (*m*, 4H), 3.00 (*s*, 3H), 3.05 (*s*, 3H), 3.49 (*m*, 2H), 3.60 (*t*, 2H), 3.95 (*dd*, 1H), 4.01 (*t*, 2H), 4.35 (*dd*, 1H), 5.49 (*m*, 1H). $^{13}$C NMR (CDCl3): δ13.79, 22.44, 22.76, 24.42, 24.50, 28.85, 28.89, 29.05, 29.07, 29.10, 29.24, 29.26, 29.37, 29.40, 31.67, 33.59, 33.88, 50.57, 51.10, 63.03, 63.53, 63.81, 64.30, 65.31, 172.70, 173.29. MALDI-TOF calculated for [$C_{32}H_{63}NO_8S$] (m/z): 621.43, observed: [M+H] 622.91. Elemental analysis for [$C_{32}H_{63}NO_8S$]: C, 61.80; H, 10.21; N, 2.25; S, 5.16. Found: C, 61.52; H,9.85; N,2.13; S, 5.03.

**DCAS (3f)**. Yield: 65%. $^1$H NMR (CDCl3): δ0.90 (*t*, 6H), 1.29 (*m*, 24H), 1.60 (*m*, 4H), 2.27 (*m*, 2H), 2.35 (*m*, 4H), 3.21 (*s*, 3H), 3.29 (*s*, 3H), 3.70 (*m*, 3H), 3.96 (*dd*, 1H), 4.13 (*t*, 3H), 4.51 (*dd*, 1H), 5.64 (*m*, 1H). $^{13}$C NMR (CDCl3): δ14.10, 22.70, 24.74, 24.84, 29.19, 29.36, 29.49, 31.91, 33.94, 34.25, 51.10, 51.64, 63.39, 63.61, 63.84, 64.56, 65.84, 172.83, 173.25. MALDI-TOF calculated for [$C_{28}H_{55}NO_8S$] (m/z): 565.37, observed: [M+H] 566.72. Elemental analysis for [$C_{28}H_{55}NO_8S$]: C, 59.44; H, 9.80; N, 2.48; S, 5.67. Found: C, 59.32; H, 9.67; N, 2.46; S, 5.63.

4. Elemental analysis.

Dry lipid samples (10 mg) were submitted to the Microanalytical Laboratory at the University of California Berkeley for elemental analysis determinations using an ICP Optima 7000 DV instrument.

5. Differential Scanning Calorimetry.

DSC experiments were based upon a protocol described in Huang and Szoka.{Huang:2008iy} Lipids films were prepared in glass tubes from a 20 mg/mL stock solution in 25% methanol in

chloroform by concentrating the lipids under vacuum. The lipid films were then rehydrated at 20 mM in 10 mM HEPES buffer containing either 150 mM NaCl, 1M NaCl, 1M NaI or 1 M $NaClO_4$.

In all experiments, the lipids were heated to 90 °C for 10 min and sonicated with heating for 10 minutes, then 250 uL of lipid was transferred to a reusable Hestelloy sample ampoule using a glass syringe. Data were collected over a range of 10-110 °C at 1 °C/min with the relevant buffer as the reference. The CpCalc 2.1 software package was used to convert the raw data into a molar heat capacity. The data was then exported to Excel and GraphPad Prism for processing. Samples were scanned through a heat-cool-heat cycle and data was collected from the second heating cycle.

6. Transmission electron microscopy.

A 2.0 uL drop of liposomes were adsorbed for 60 s on glow-discharged carbon-coated copper grid (Ted Pella, Redding, CA) and water was wicked off. Then, 2 microliters of a 1% uranyl acetate negative stain solution was added and left to stain for 60 s and wicked off. The grid was then washed with double deionized water three times and the water was removed by wicking. Grids were imaged with an FEI Tecnai T12 TEM (FEI company, Hillsboro, OR) at 120kV. Data were acquired with a 4 x 4 Gatan UltraScan CCD camera (Gatan, Pleasanton, CA).

7. Small angle X-ray scattering measurements.

Pure lipids for SAXS were prepared at 20 mM in 10mM HEPES buffer containing 150 mM NaCl. Aqueous phases were heated to 90 °C and added to lipid, vortexed and sonicated in a sonicating bath for 10 min. SAXS data were measured on the SAXS/WAXS beamline at the Australian Synchrotron. Buffer was drawn into a fixed position flowthrough quartz capillary, mounted in a brass block fitted with a thermocouple, to allow for background measurements and the temperature ramped

from 'nominal' 20 °C to about 80 °C, and a 10 min equilibration at each temperature prior to acquisition of scattering for 5 sec. The camera (Pilatus 1M) was positioned 3252 mm from the sample, with X-ray energy selected at 11 keV. Modeling of scattering data calculations were performed using GIFT.

**Table S1**: Elemental analysis of AS lipids.

| | | C% | H% | N% | S% |
|---|---|---|---|---|---|
| **DCAS** | Expected | 59.44 | 9.80 | 2.48 | 5.67 |
| | Observed | 59.32 | 9.67 | 2.46 | 5.63 |
| **DLCS** | Expected | 61.80 | 10.21 | 2.25 | 5.16 |
| | Observed | 61.52 | 9.85 | 2.13 | 5.35 |
| **DMCS** | Expected | 63.68 | 10.69 | 2.06 | 4.72 |
| | Observed | 63.52 | 10.92 | 1.98 | 5.35 |
| **DPCS** | Expected | 65.35 | 10.97 | 1.91 | 4.36 |
| | Observed | 65.17 | 11.33 | 1.95 | 4.79 |
| **DSCS** | Expected | 66.79 | 11.21 | 1.77 | 4.05 |
| | Observed | 66.58 | 11.54 | 1.74 | 4.65 |
| **DOAS** | Expected | 67.22 | 10.64 | 1.78 | 4.08 |
| | Observed | 67.22 | 10.9 | 1.68 | 4.33 |

**Figure S1**: $BrPrOSO_3$–DIPEA (1) – $^1H$ NMR

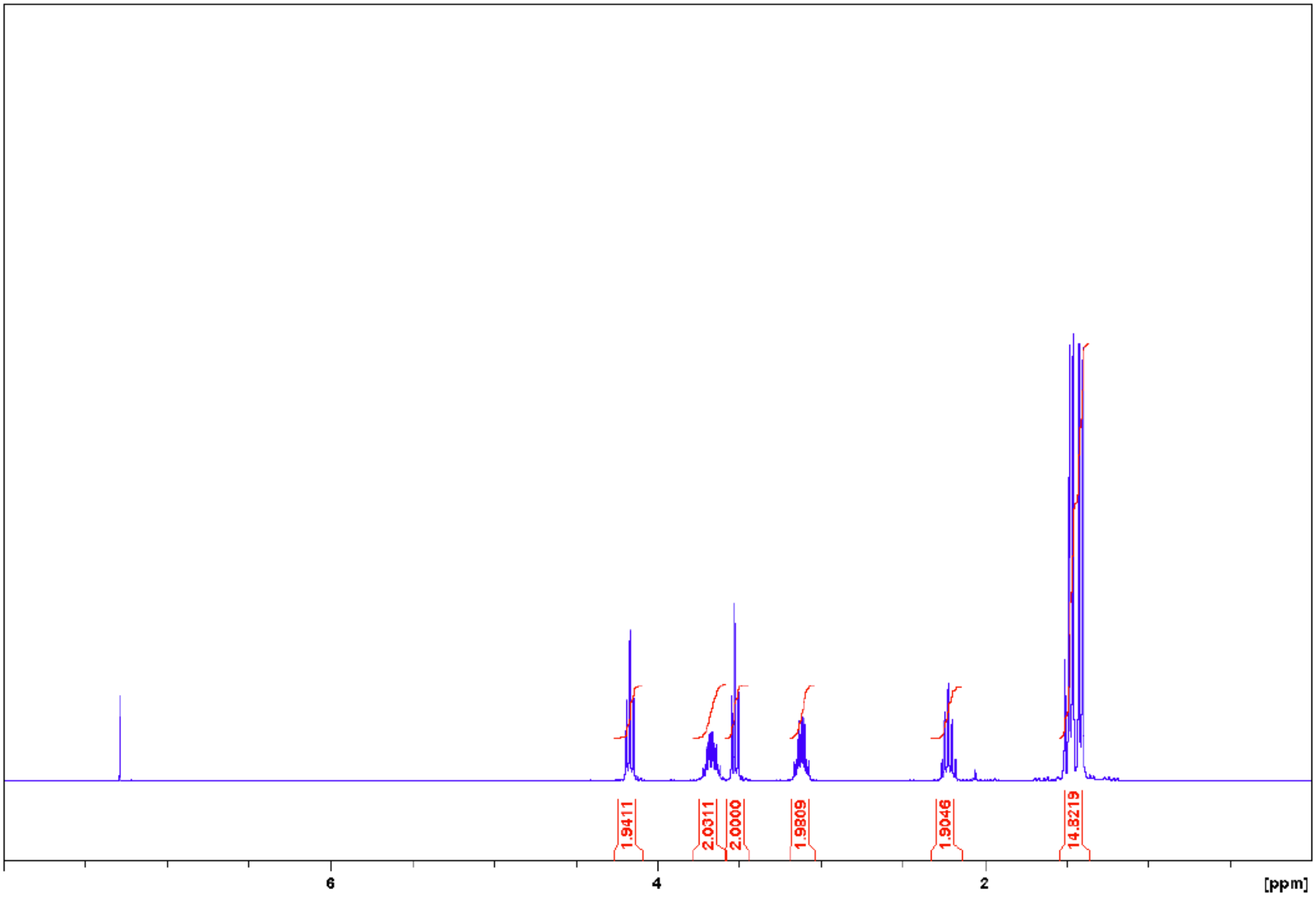

**Figure S2**: $BrPrOSO_3$-DIPEA (1) – $^{13}C$ NMR

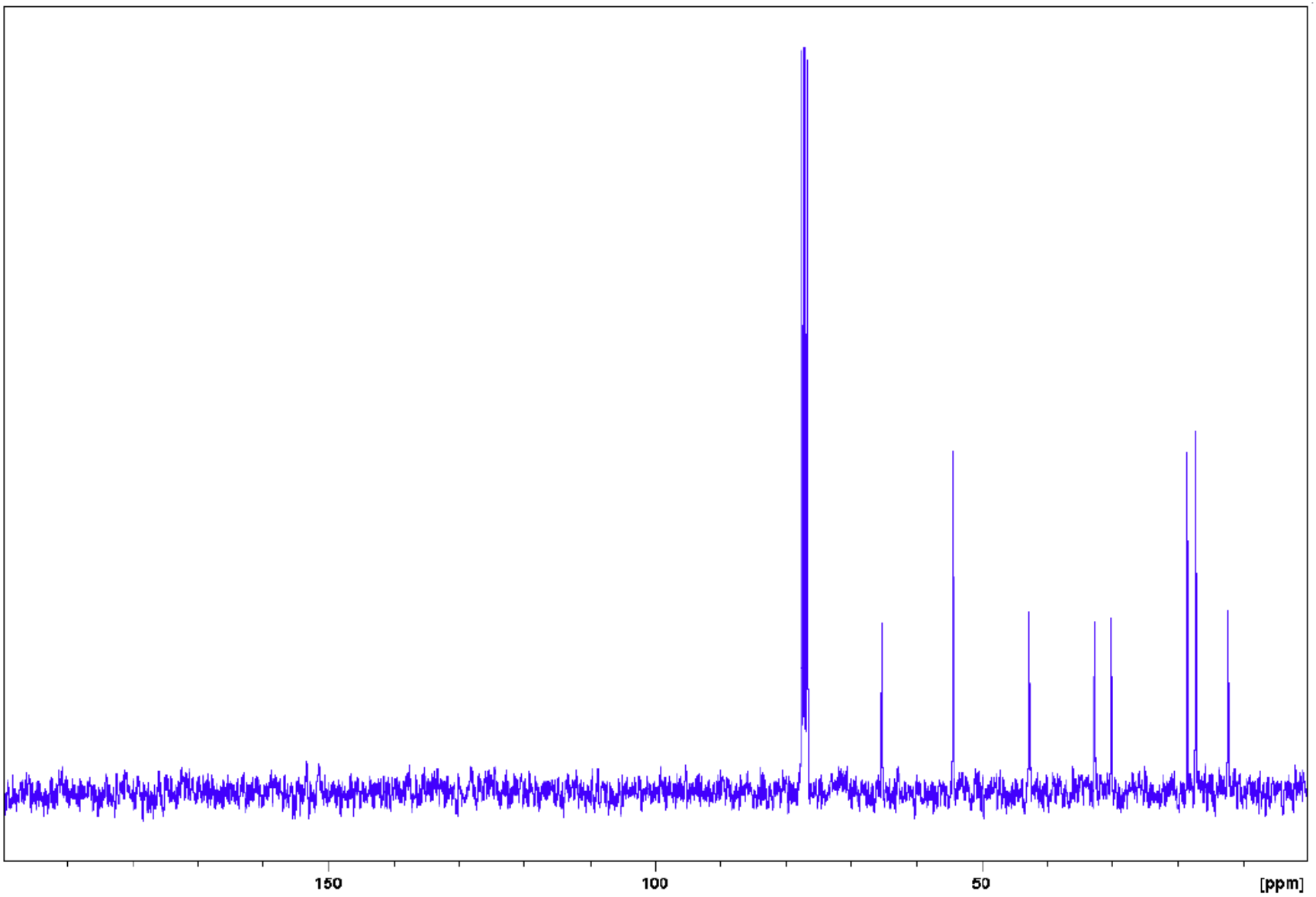

**Figure S3**: DOAS (**3a**) – $^{1}$H NMR

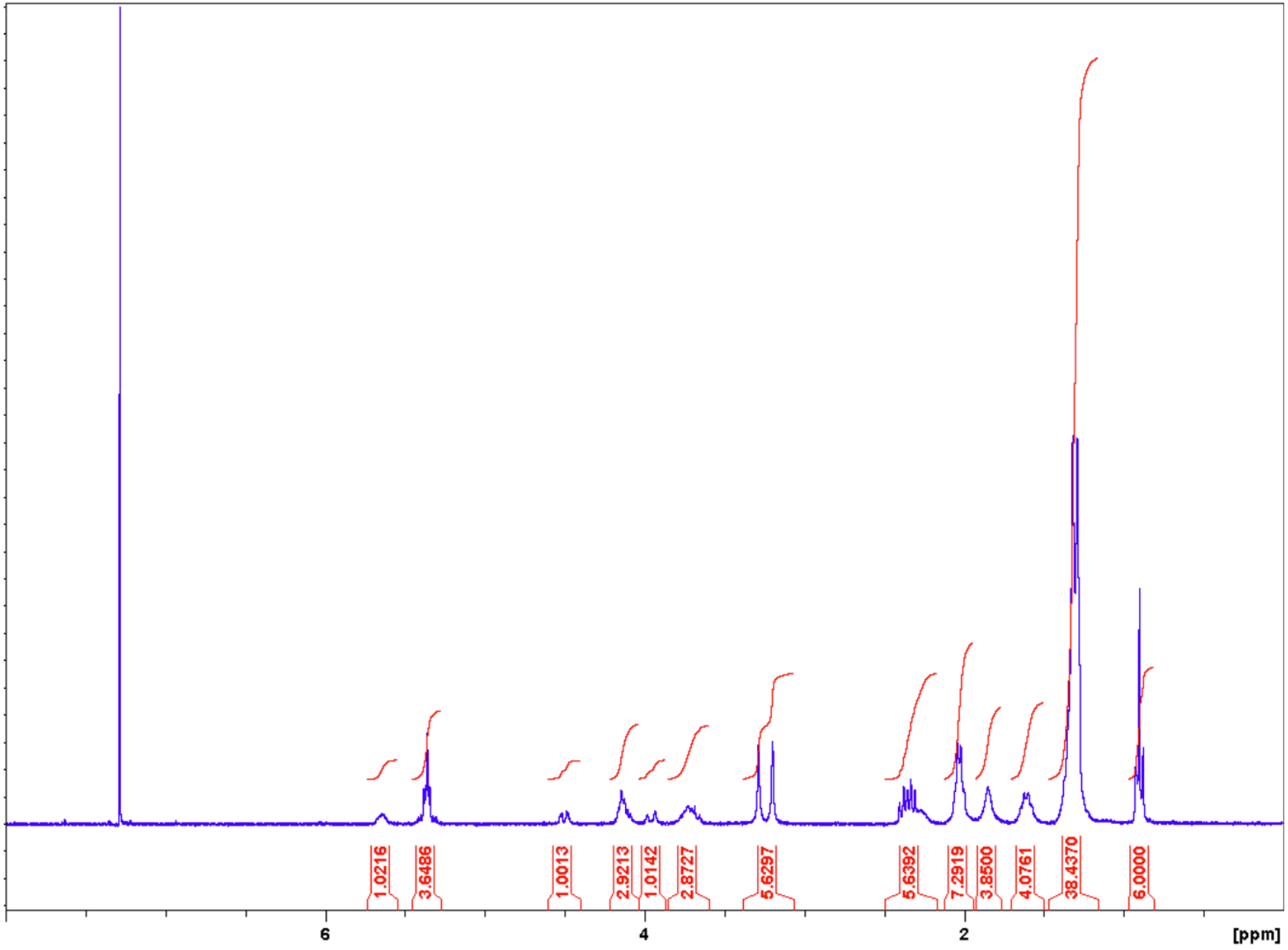

**Figure S4**: DOAS (**3a**) – $^{13}C$ NMR

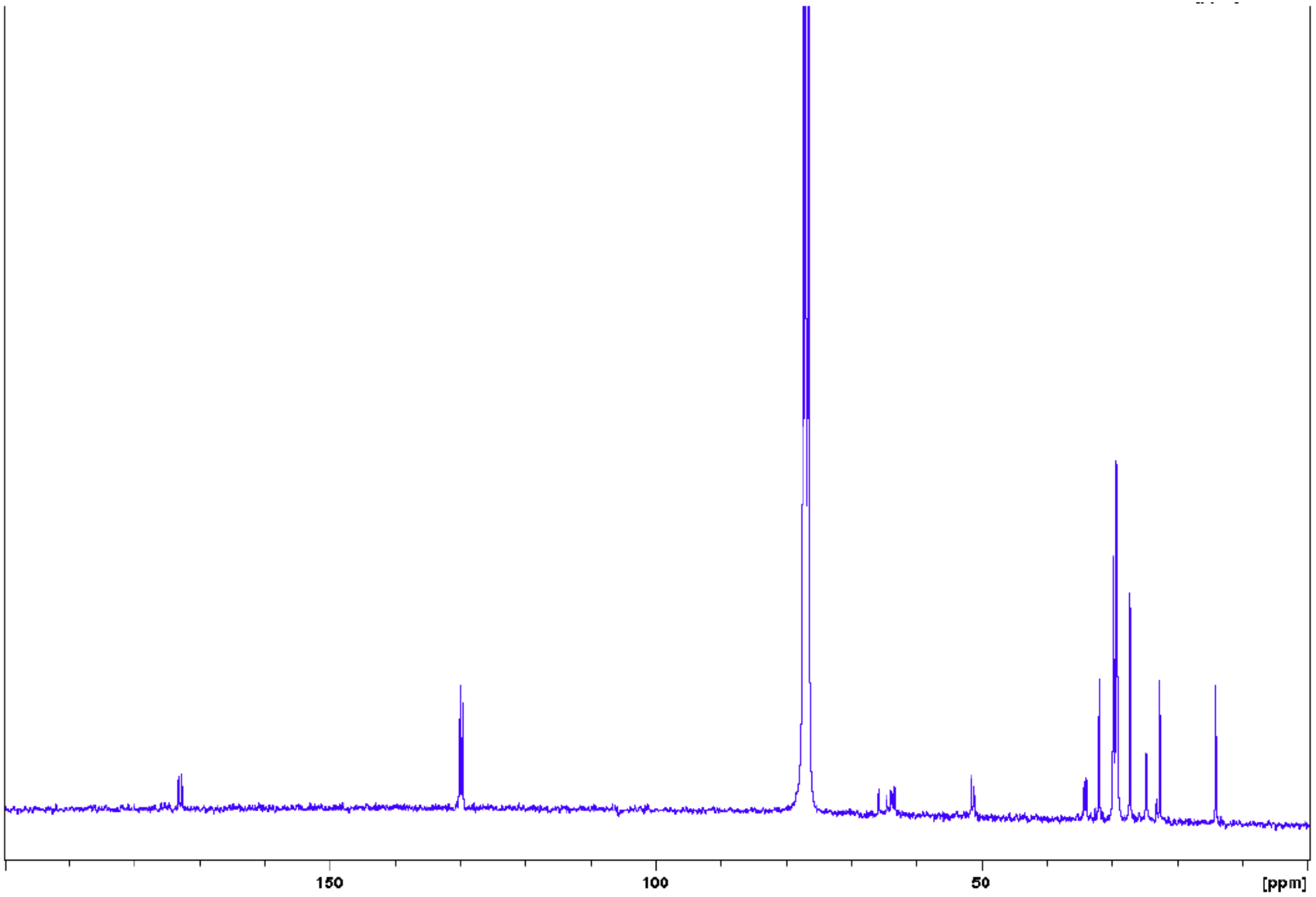

**Figure S5**: DSAS (**3b**) – $^{1}$H NMR

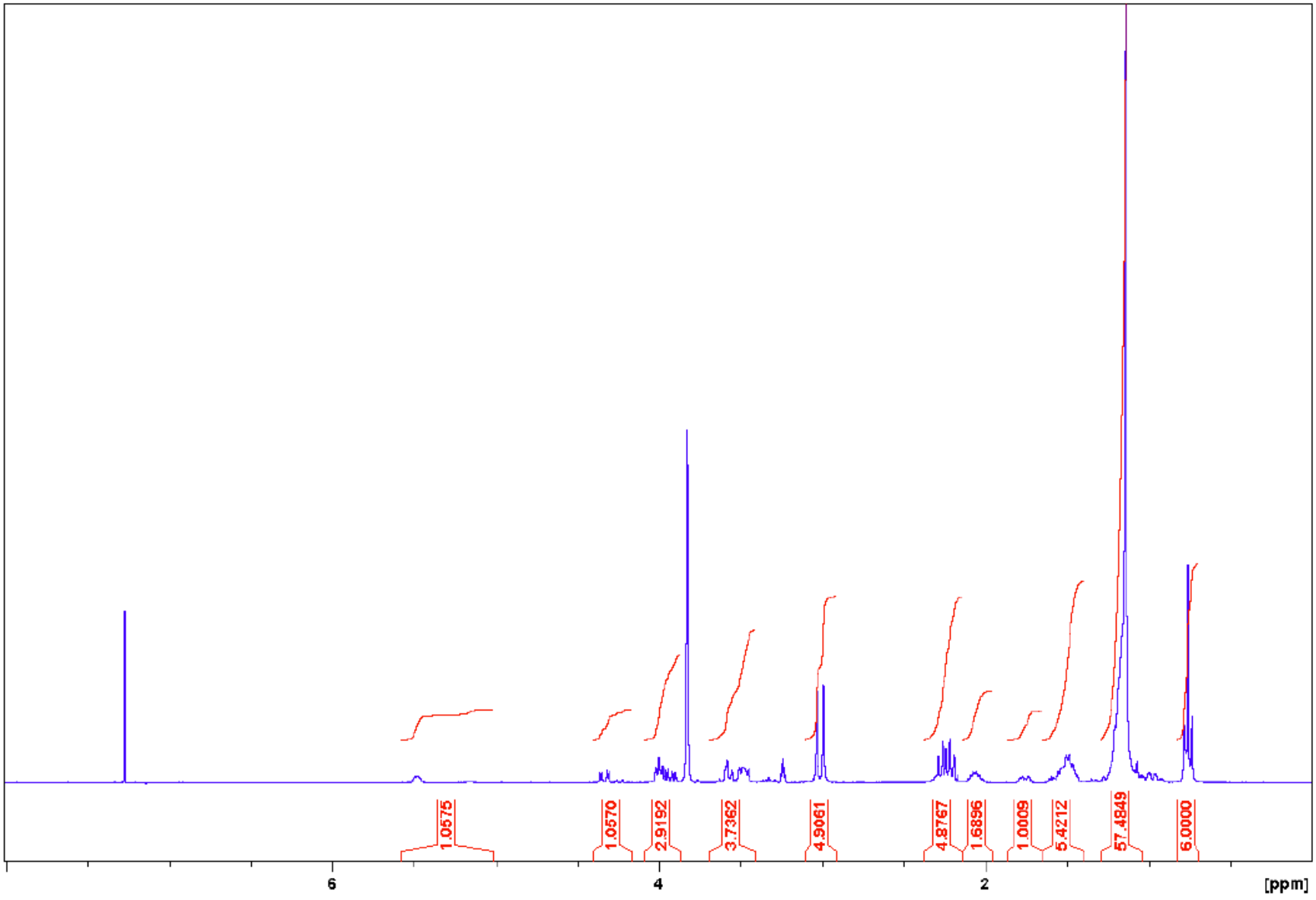

**Figure S6**: DSAS (**3b**) – $^{13}C$ NMR

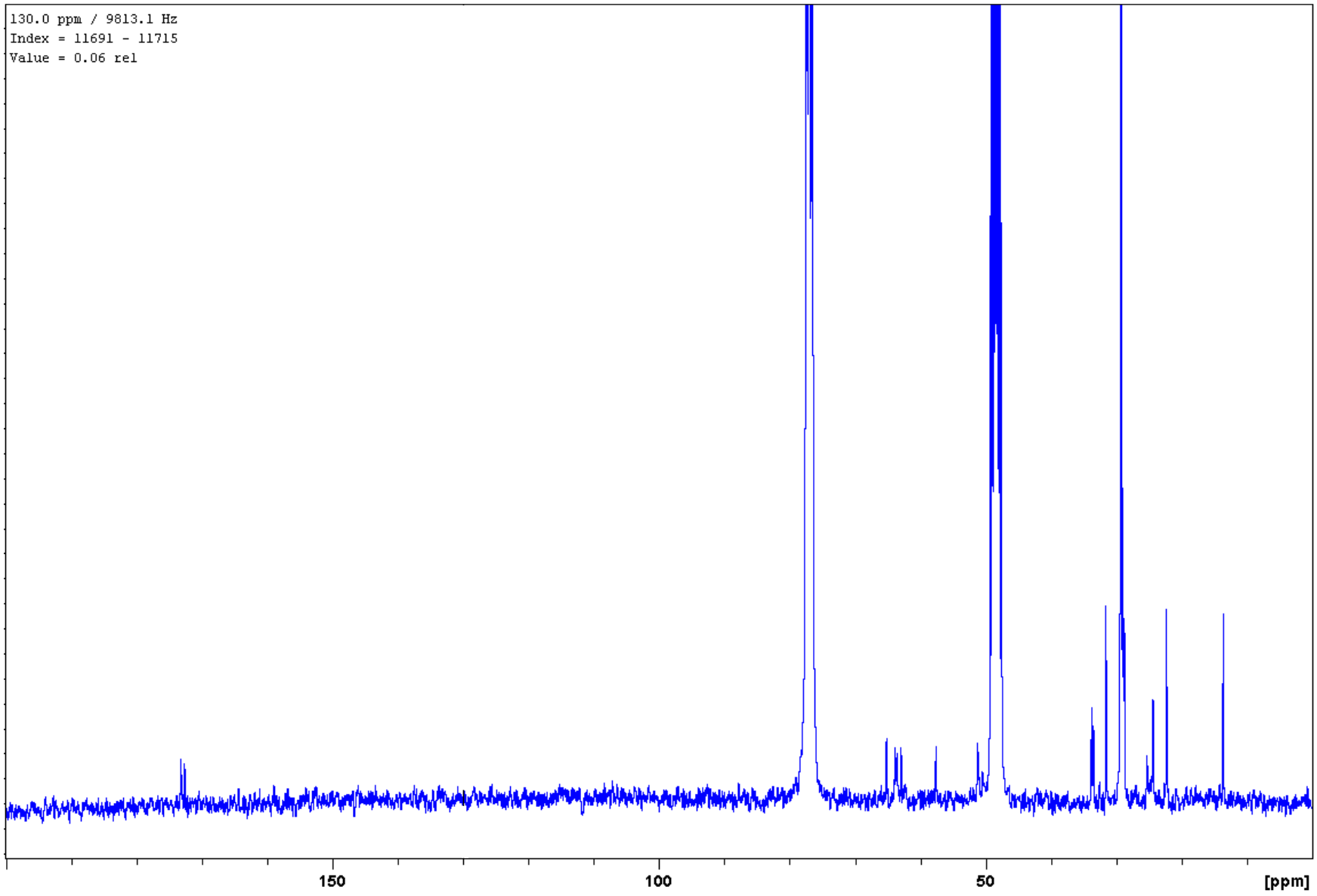

**Figure S7**: DPAS (**3c**) – $^{1}$H NMR

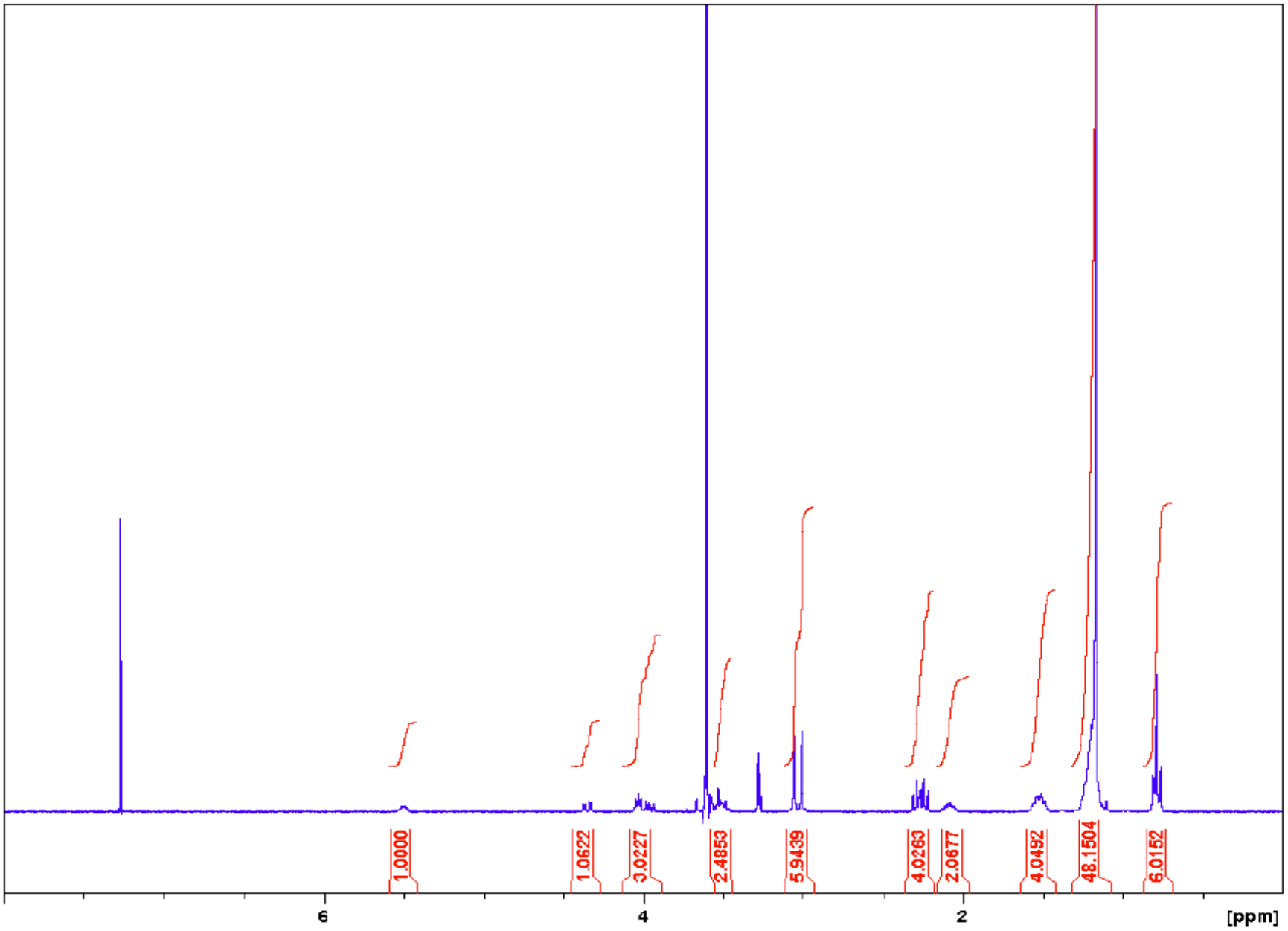

**Figure S8**: DPAS (**3c**) – $^{13}C$ NMR

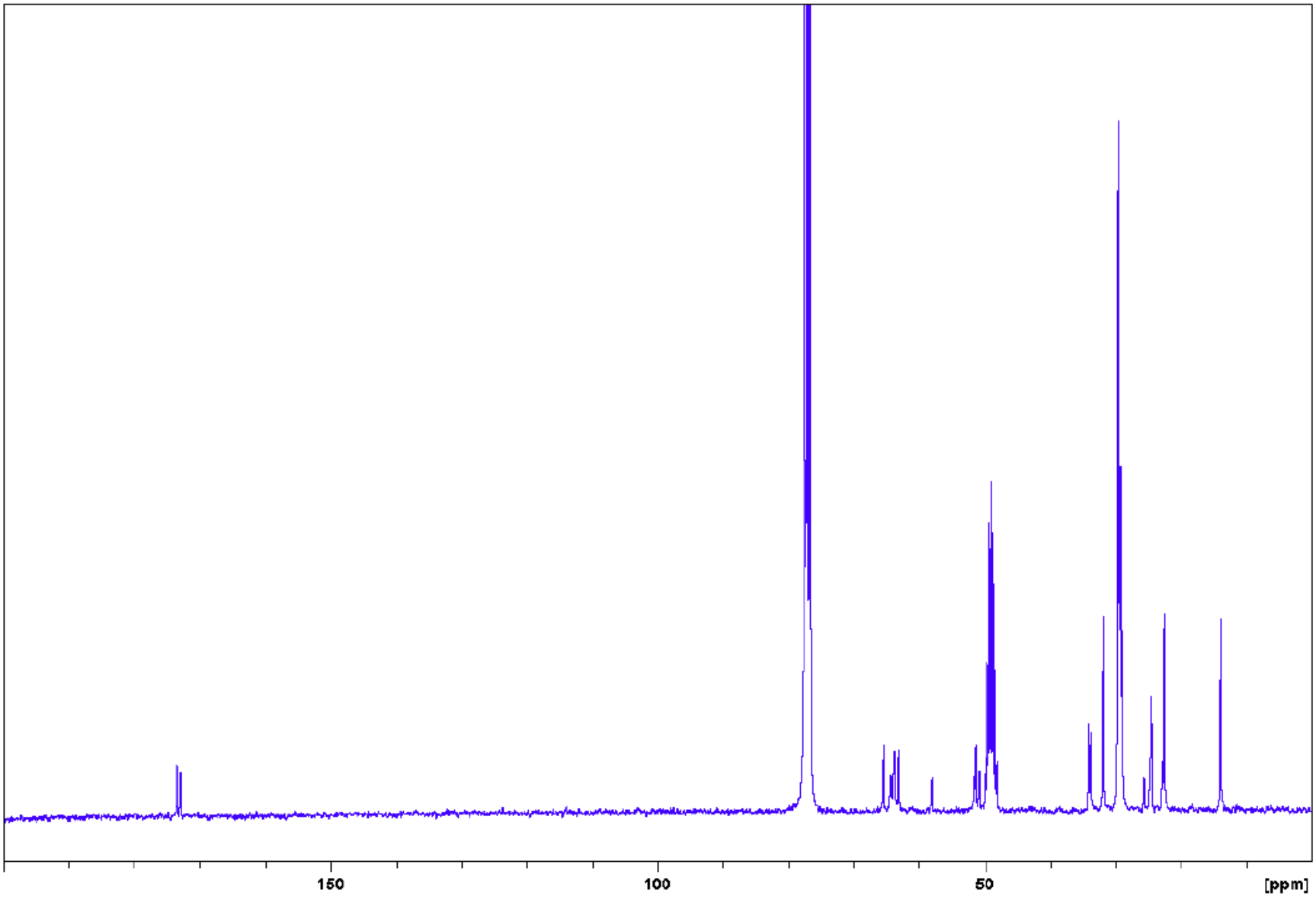

**Figure S9**: DMAS (**3d**) – $^{1}$H NMR

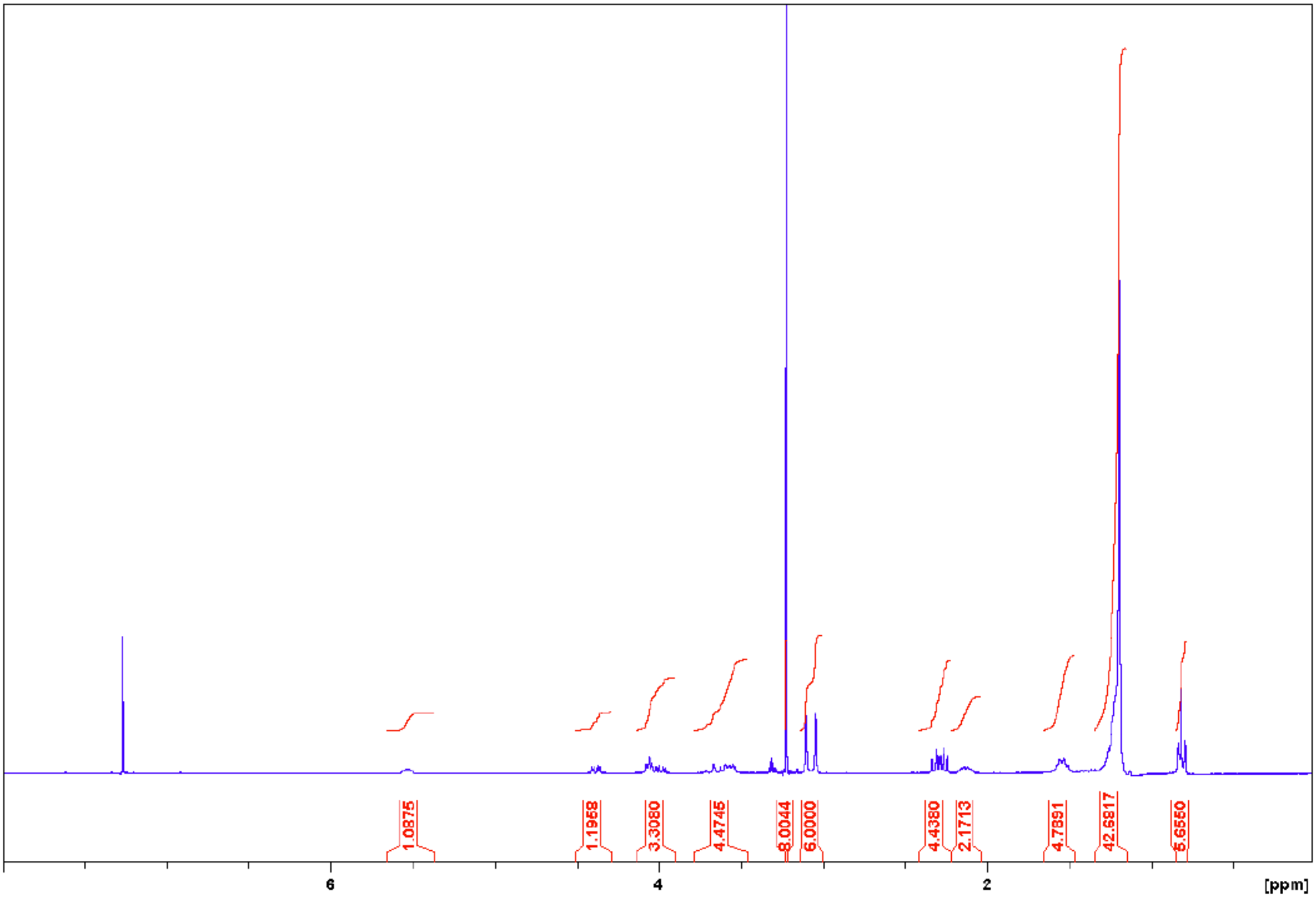

**Figure S10**: DMAS (**3d**) – $^{13}C$ NMR

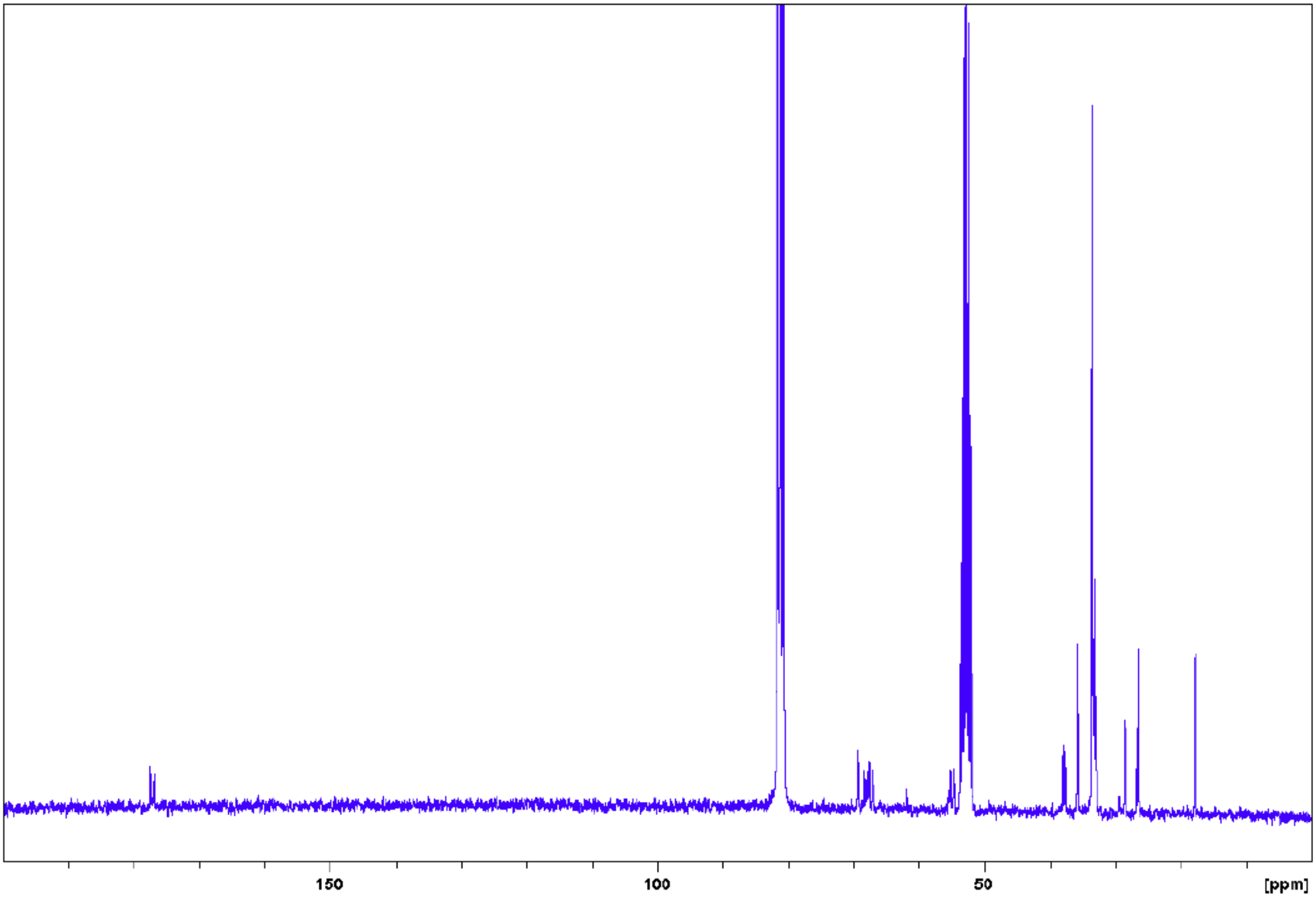

**Figure S11**: DLAS (**3e**) – $^{1}$H NMR

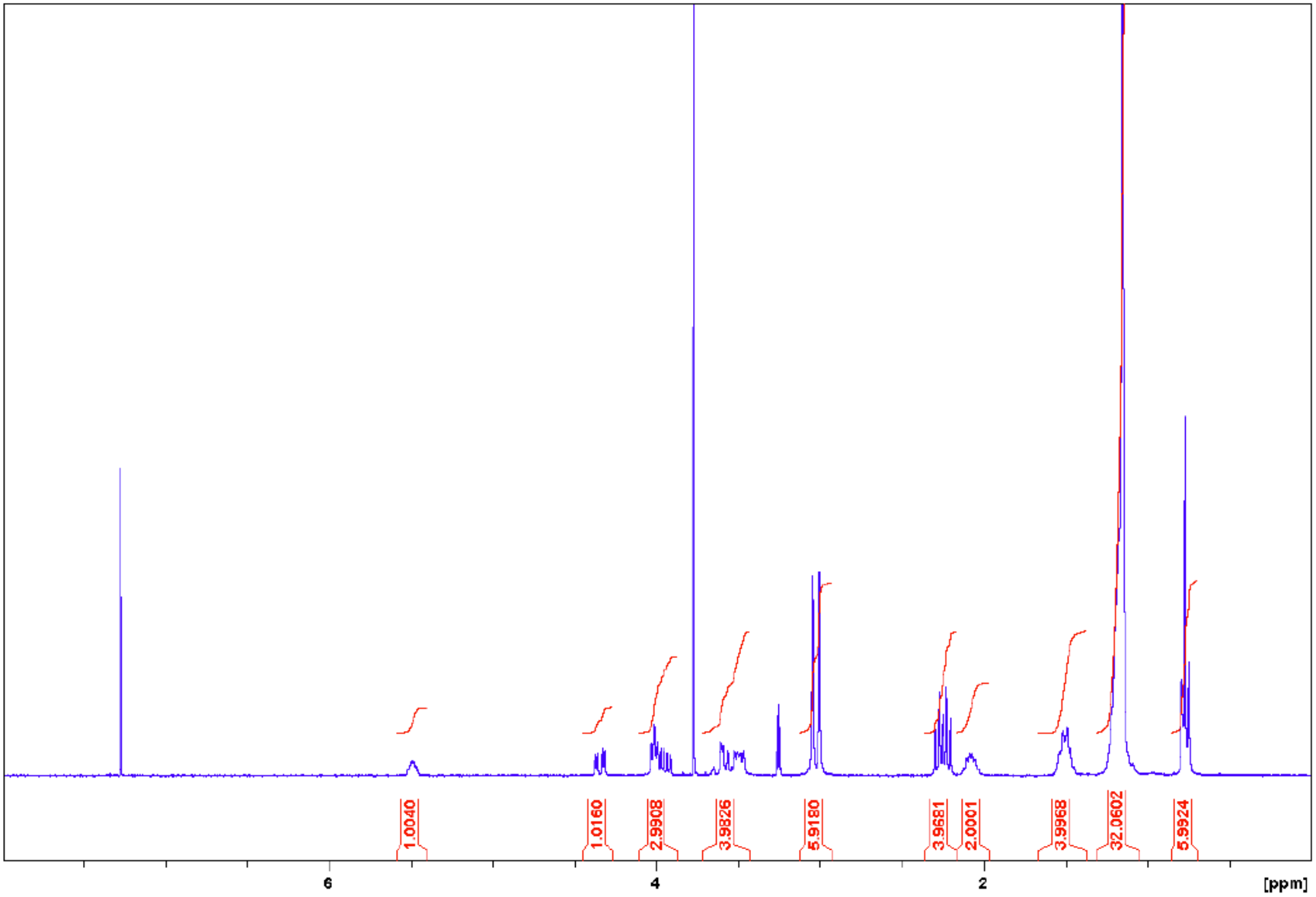

**Figure S12**: DLAS (**3e**) – $^{13}C$ NMR

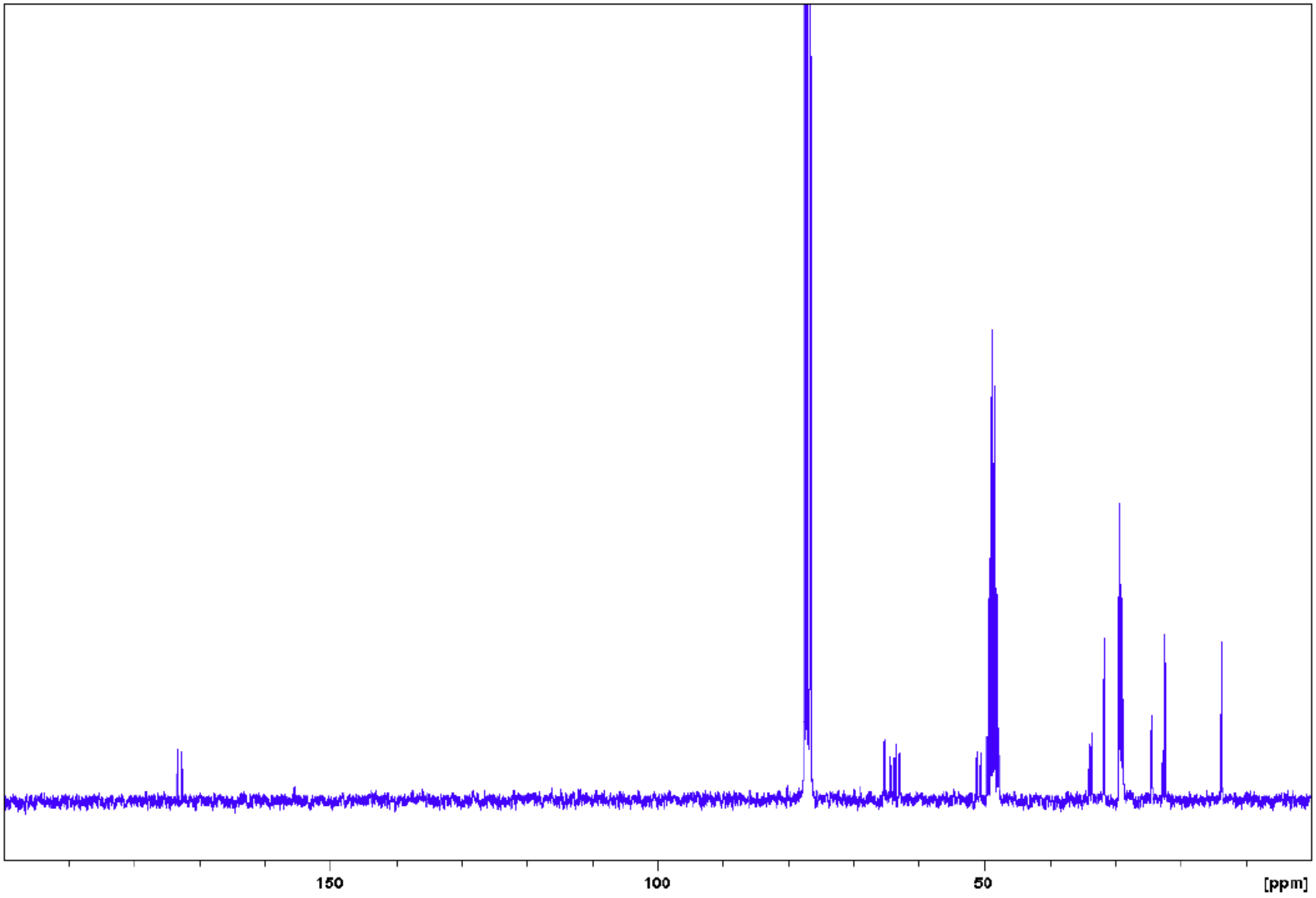

**Figure S13**: DCAS (**3f**) – $^{1}$H NMR

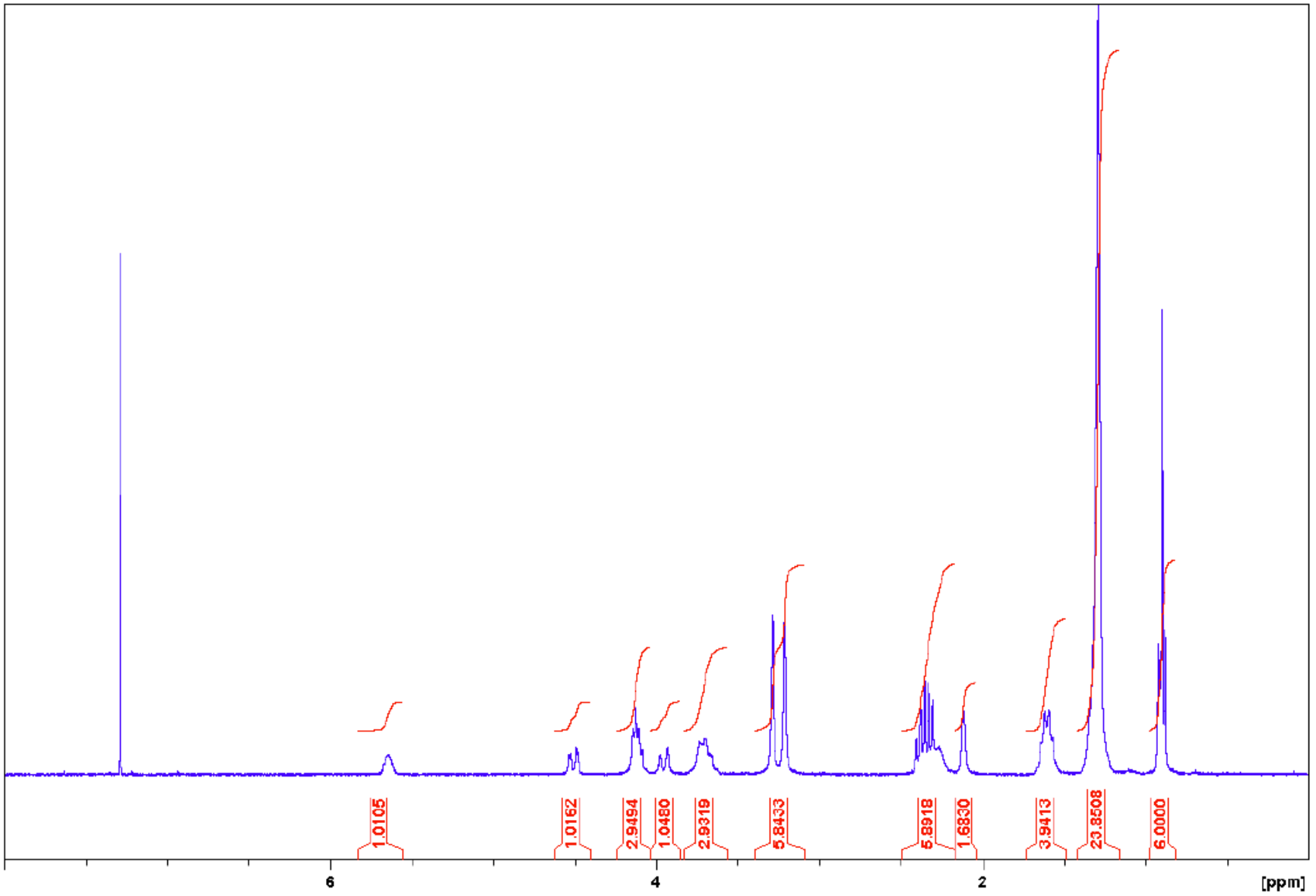

**Figure S14**: DCAS (**3f**) – $^{13}C$ NMR

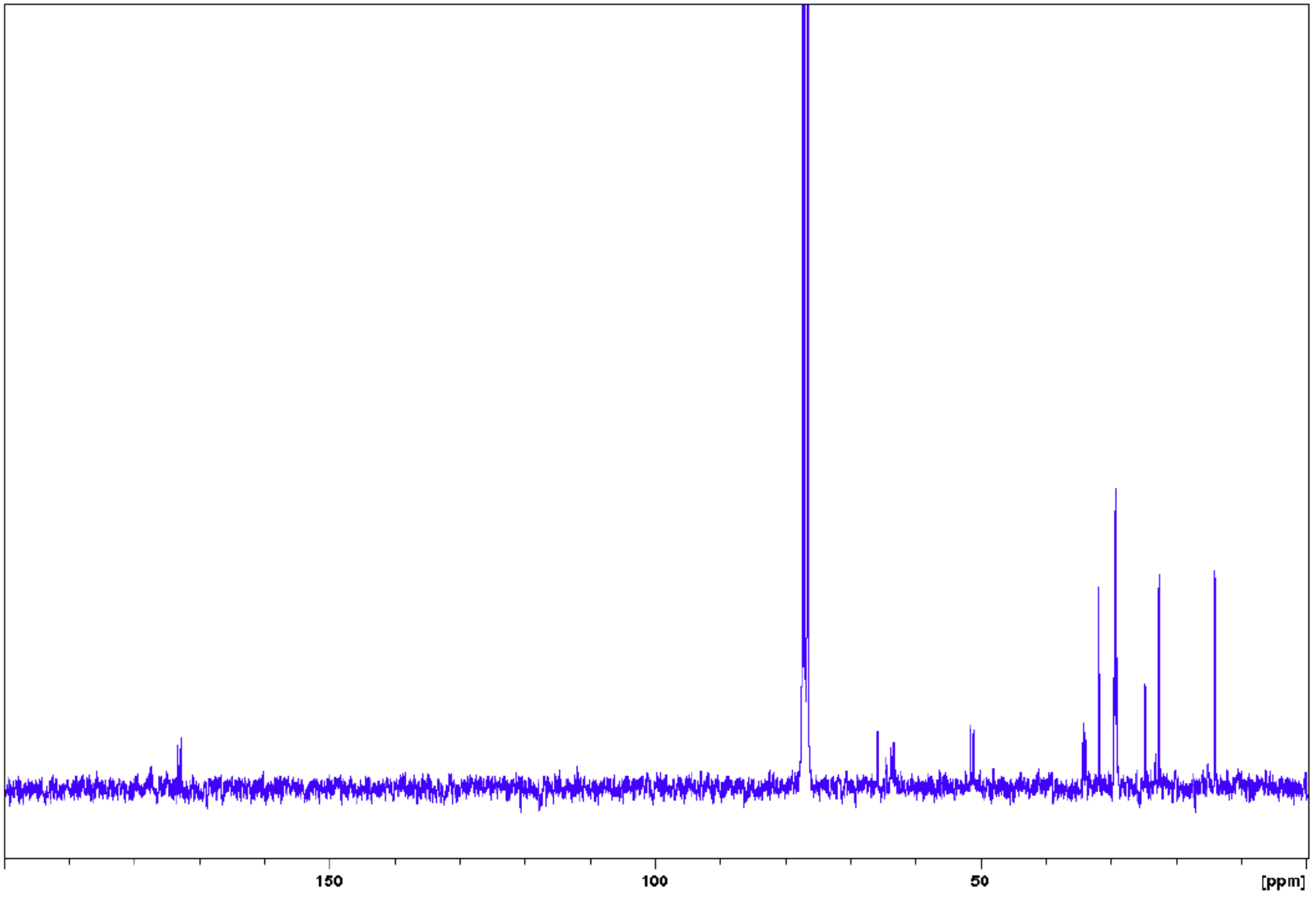

**Figure S15**: SAXS scattering profile for DOAS (3a) with increasing temperature (background subtracted).

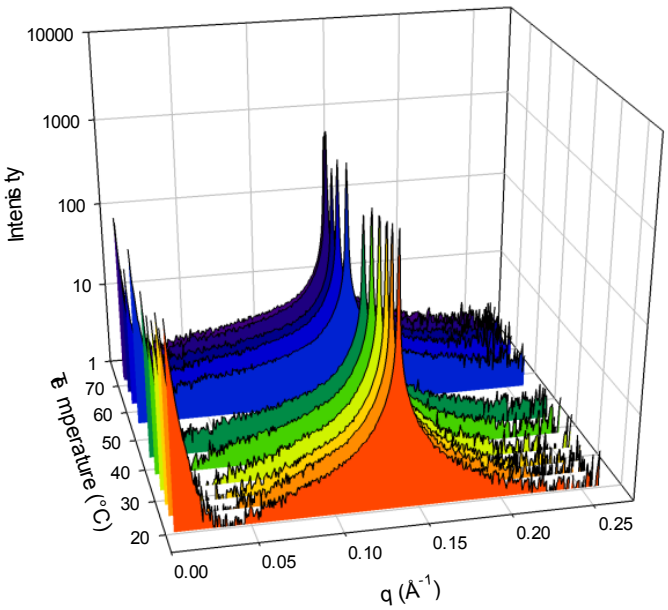


**Figure S16**: DOAS (3a) scattering profile with increasing temperature.

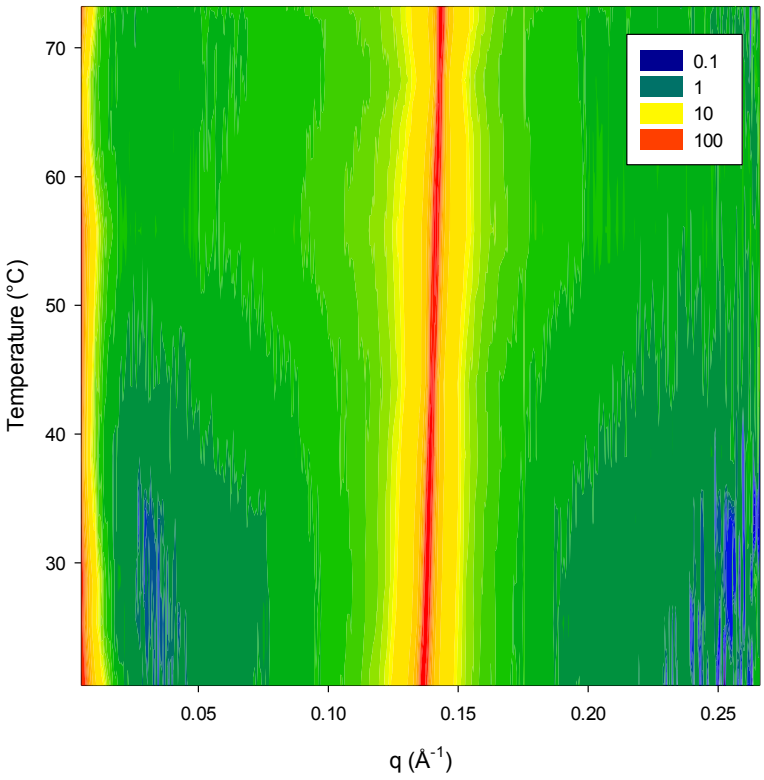

**Figure S17**: Change in lamellar spacing with temperature for DOAS (3a).

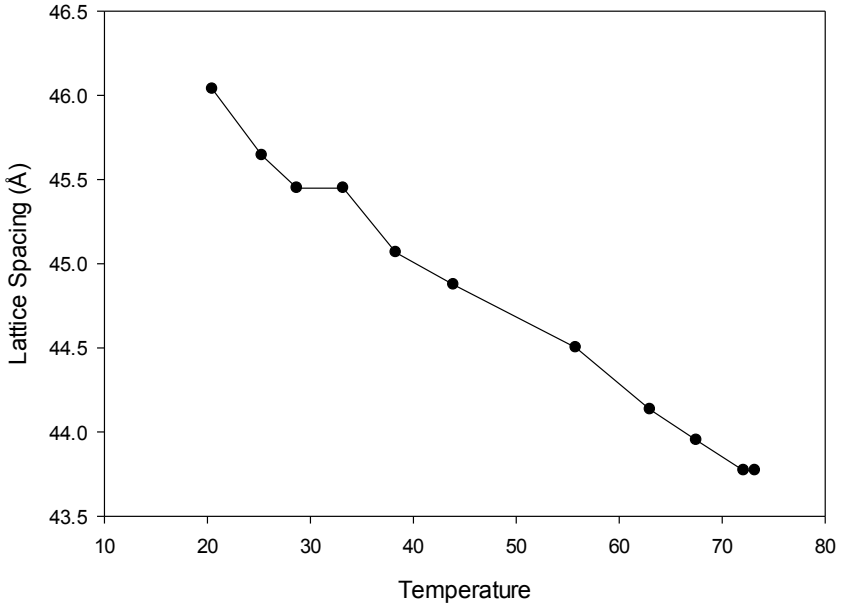


**Figure S18**: DOAS (3a) SAXS data and fit for the thickness pair distance distribution function at 20 °C. Structure factor for the lamellar phase (modified Caille Theory) number of bilayer: 200, bilayer spacing: 46.0 Å, Caille parameter: 0.14 Å$^{-1}$.

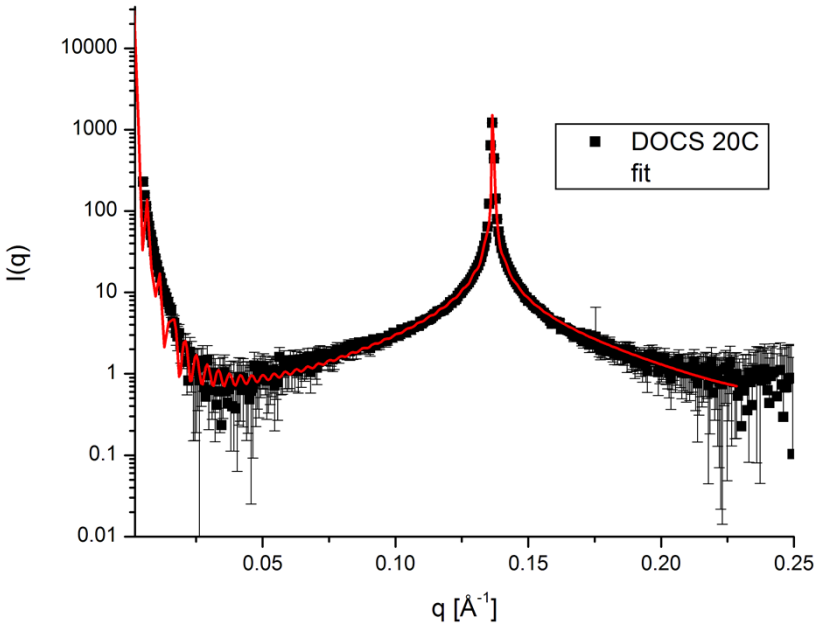

**Figure S19**: pt(r) calculated from SAXS data in Figure S18.

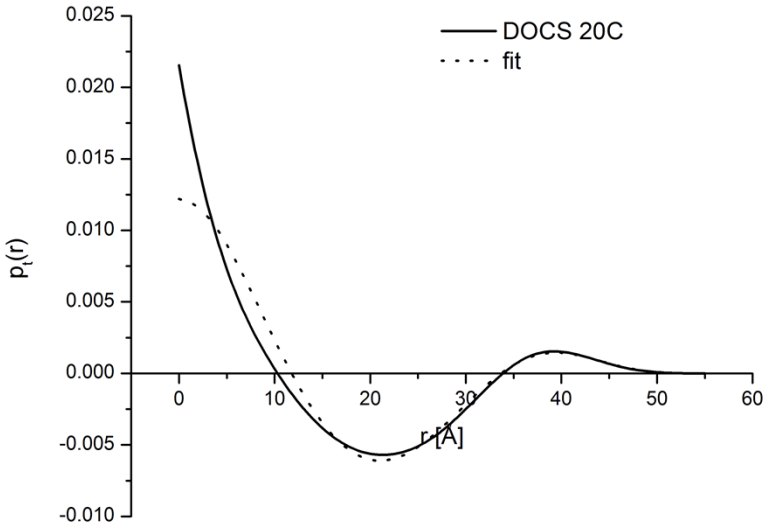


**Figure S20**: DOAS (3a) SAXS data and fit for the thickness pair distance distribution function at 80 °C. Structure factor for the lamellar phase (modified Caille Theory) number of bilayer: 76.3, bilayer spacing: 43.8 Å, Caille parameter: 0.14 Å$^{-1}$.

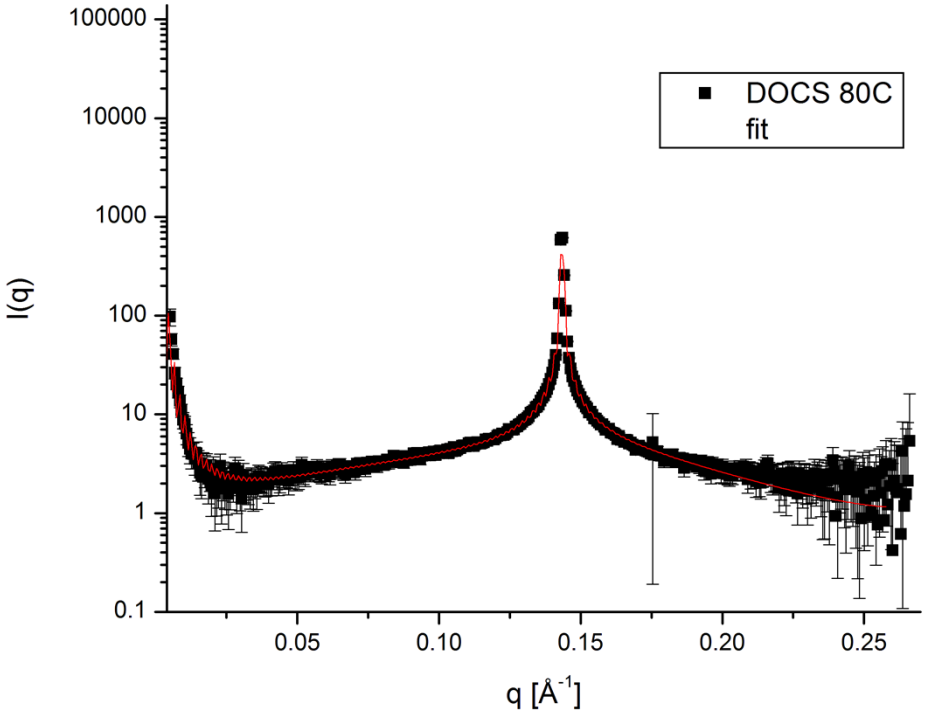

**Figure S21**: pt(r) calculated from SAXS data in Figure S20.

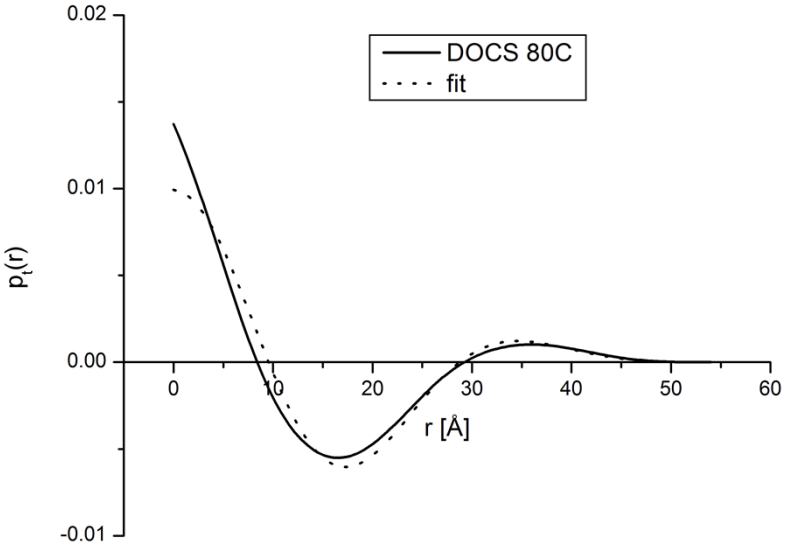


**Figure S22**: Electron density within the bilayer thickness calculated via deconvolution of the pt(r) functions.

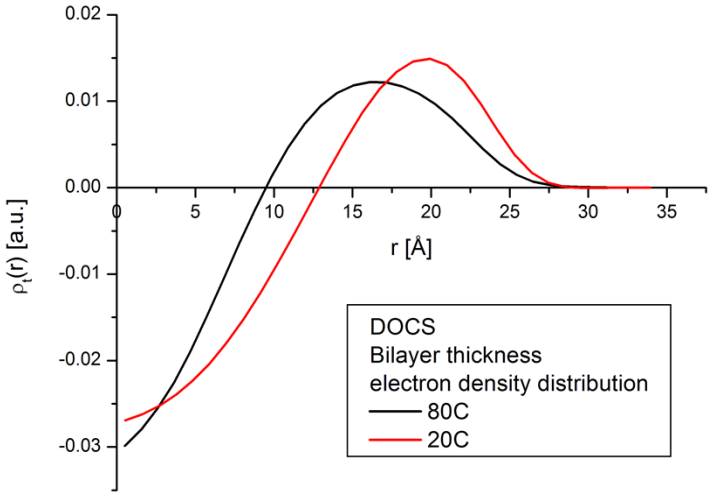

**Figure S23**: SAXS scattering profile for DMAS (3d) with increasing temperature.

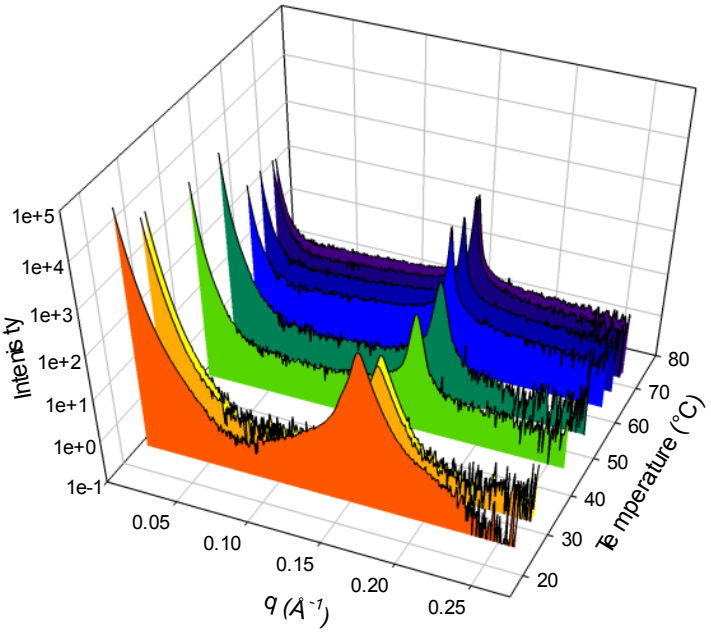


**Figure S24**: DMAS (3a) scattering profiles with increasing temperature.

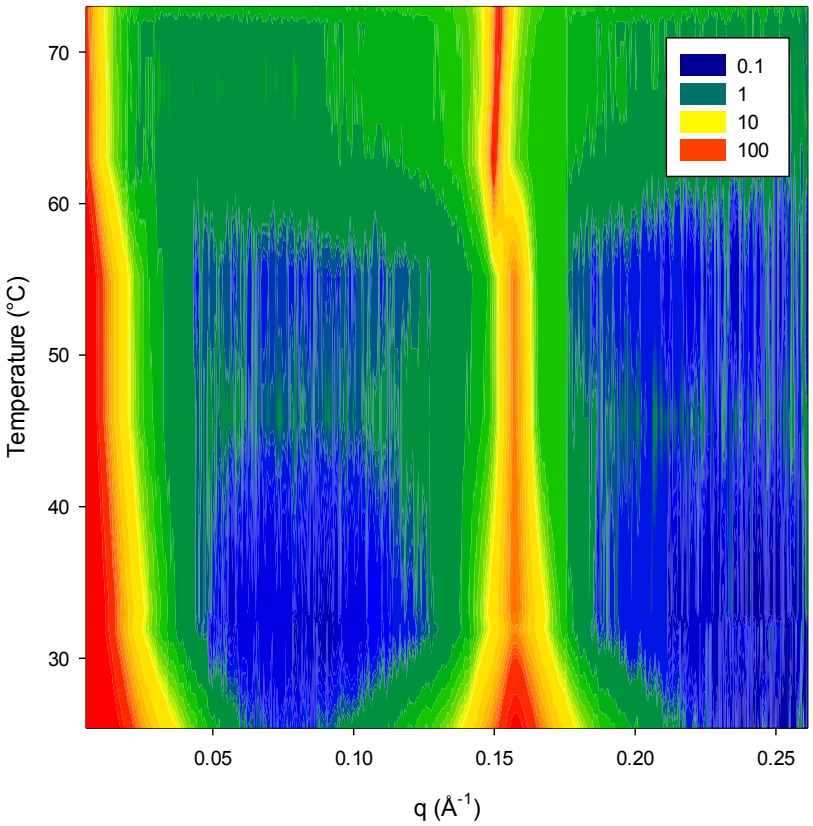

**Figure S25**: Determination of particle size by dynamic light scattering with increasing temperature. The high polydispersity index of these measurements are shown in Figure S26.

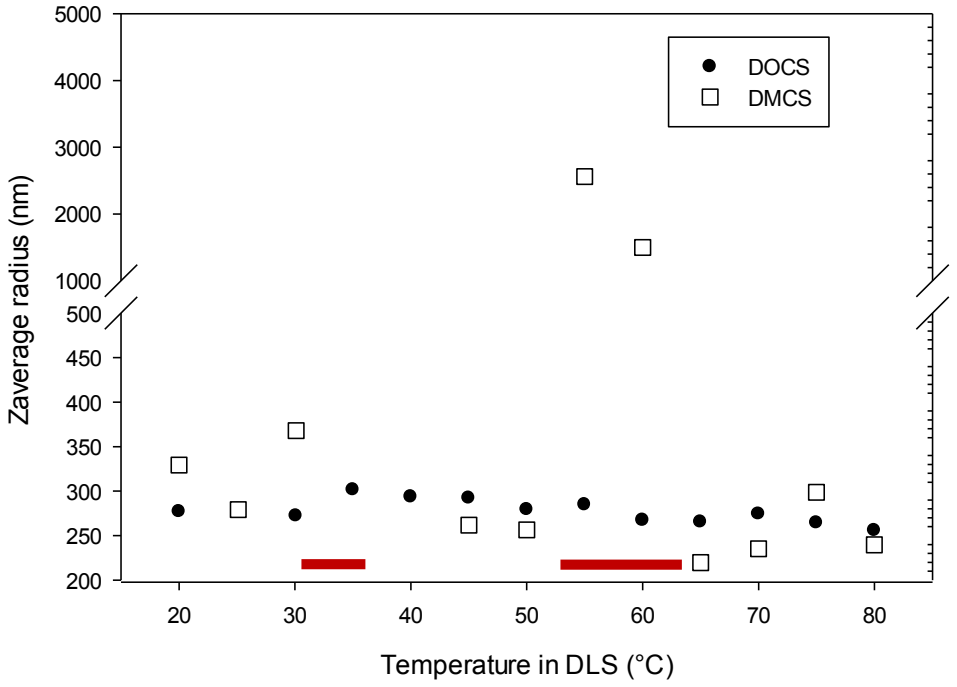


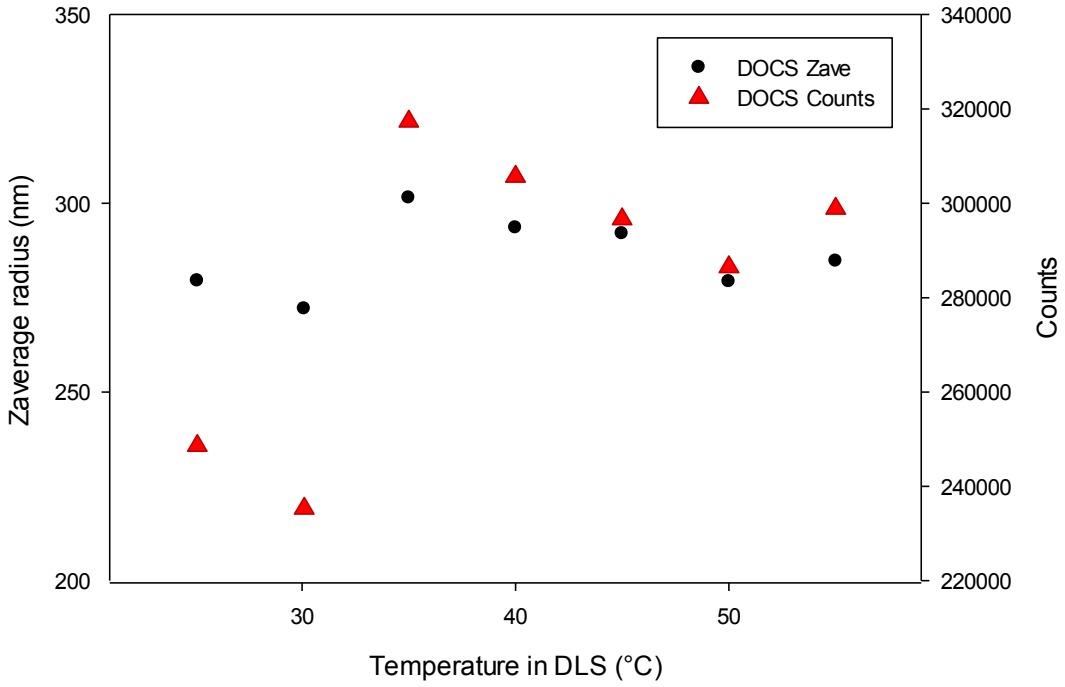

**Figure S26**: Determination of polydispersity by dynamic light scattering with increasing temperature for DMAS.

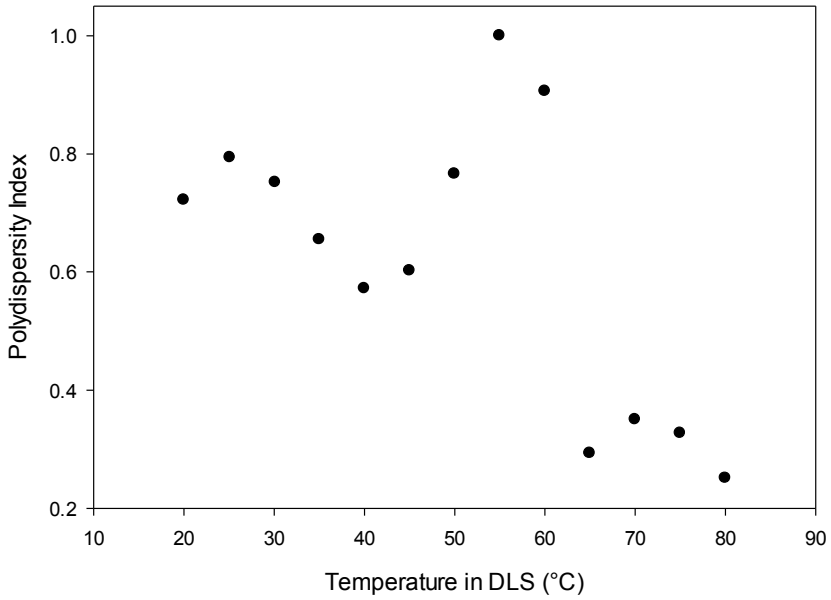


**Figure S27**: Differential scanning calorimetry of DMAS in the presence of kosmotropic salts as compared to DMPC.